# Superpave In-Situ Stress/Strain Investigation – Phase II

# Implementing SISSI data with MEPDG

## Introduction

Accurate pavement performance prediction is widely recognized as one of the most complex and difficult tasks to accomplish. The importance of such a goal cannot be over-emphasized as reliable predictions make it possible to modify design or construction to improve performance, potentially resulting in the saving of millions of dollars. Proper selection of pavement materials and layer thicknesses can be optimized using performance-based specifications. The basic requirement is the availability of an accurate pavement performance prediction methodology.

Many highway agencies use the current AASHTO Guide for Design of Pavement Structures to design their pavement systems. The limitation inherent in this method is the empirical nature of the decision process, which was derived from the road test conducted almost 45 years ago in Ottawa, Illinois. The AASHTO design method established a relationship between the number of load cycles, pavement structural capacity, and performance, measured in terms of serviceability. The concept of serviceability was introduced in the AASHTO method as an indirect measure of the pavement's ride quality. The serviceability index is based on surface distresses typically observed in pavements. The major advantage of these methods is the mathematical simplicity that does not require advanced computational capabilities or extensive material characterization for the design of pavement structures; however, with all of these advantages, the empirical methods are not without some serious limitations. The major limitation is that they cannot provide accurate predictions for material, environment, and traffic conditions that differ from those for which the models were originally developed. Mechanistic methods generally use the linear-elastic theory of mechanics to compute structural responses in combination with empirical models to predict number of loads to failure for flexible pavements. The dilemma is that pavement materials do not exhibit the simple behavior assumed in isotropic linear-elastic theory. Nonlinearities, time and temperature dependency, and anisotropy are some examples of complicated features often observed in pavement materials. In this case, advanced modeling is required to mechanistically predict performance.

The mechanistic design procedure is based on the theories of mechanics that relate pavement structural behavior and performance to traffic loading and environmental influences. It is well understood that the pavement responses, such as the stresses and strains in the system, are directly related to the pavement layer material properties. Thus, characterization of these materials is an important factor for the response prediction.

Progress has been made in recent years to provide solutions to isolated pieces of the mechanistic-performance prediction problem. However, the reality is that fully mechanistic methods are not yet available for practical pavement design.
The mechanistic-empirical procedure, as the name implies, includes two discrete parts: mechanistic computations and empirical models. The empirical models are used to fill in the gaps that exist between the mechanistically determined stress and strains and the developed distresses within the pavement structure. Simple mechanistic responses are easy to compute with assumptions and simplifications (e.g., homogeneous material, small strain analysis, and static loading as typically assumed in linear elastic theory), but they by themselves cannot be used to predict performance directly; some type of empirical model (transfer functions) is required to make the appropriate correlation (Newcomb et al. 1983, Timm and Newcomb 2003). Mechanistic-empirical methods are considered an intermediate step between empirical and fully mechanistic methods.

The newly released MEPDG, based on NCHRP 1-37A (ERES 2004), has adopted a mechanistic-empirical pavement design procedure in which pavement distresses are calculated through calibrated distress prediction models based on material properties determined from laboratory tests and local traffic and climate conditions. The calibrated distress prediction models are based on the critical pavement responses mechanistically calculated by a structural model and coefficients determined through national calibration efforts using the LTPP database. A great number of design input parameters related to structures, materials, environment, and traffic are required in the MEPDG to determine stresses, strains, and developed distresses. With the performance-related design concept, a pavement designer has the capability and flexibility to incorporate several design features and material properties to a certain pavement site and its conditions to meet the key distresses and smoothness performance requirements.

Conducting parametric studies is an important and useful step towards implementation of the MEPDG as a new pavement design tool by state highway agencies. The results and conclusions of such studies are useful for understanding the procedures used in MEPDG, finding weaknesses and problems within the local agencies' practices that need to be addressed, and defining priorities for the implementation and calibration tasks. The objective of the sensitivity study presented in this report is to determine the sensitivity of results from MEPDG to those specific parameters for which no data was collected at SISSI sites or uncertainty exists towards accuracy of measurements. Identified sensitive parameters will be used to develop a probabilistic-based approach for performance predictions.

## Overview of MEPDG

The various versions of the AASHTO Pavement Design Guide have served the pavement engineering community well for several decades. However, the low traffic volumes, dated vehicle characteristics, short test duration, narrow range of material types, single climate, and other limitations of the original AASHTO Road Test have called into question the continuing use of the empirical AASHTO Design Guide as the nation's primary pavement design procedure. These perceived deficiencies were the motivation for the development of MEPDG. The MEPDG provides a state-of-the-practice tool for the design of new and rehabilitated pavement structures based on mechanistic-empirical principles. Because the mechanistic procedures are able to better account for climate, aging, present-day materials, and present-day vehicle loadings; variation in performance, in relation to design life, should be reduced. This capability will reduce life cycle costs significantly over an entire highway network.

At present, the only comprehensive documentation for the MEPDG available to the general public is the Web-based version provided by the Transportation Research Board at http://www.trb.org/mepdg/. Version 1.0 of the MEPDG software is also available for downloading from this site. An independent review of NCHRP 1-37A was conducted by NCHRP under project 1-40 and was completed by September 2006. The independent review has resulted in a number of improvements, many of which are being incorporated into the MEPDG under NCHRP Project 1- 40.

In this section, a brief review of some key considerations and features in the MEPDG, focusing on flexible pavements, is provided.

## General Considerations

The MEPDG considers truck traffic loadings in terms of the full axle load spectra: single, tandem, tridem, and quad axles. The equivalent single axle load (ESAL) concept is no longer used as a direct design input. The MEPDG considers the number of heavy trucks as an overall indicator of the magnitude of truck traffic loadings (FHWA class 4 and above).

Environmental conditions have a significant effect on the performance of flexible pavement. The interaction of the climatic factors with pavement materials and loading is complex. Factors such as precipitation, temperature, freeze-thaw cycles, and water table depth affect pavement and subgrade temperature and moisture content, which, in turn, directly affect the load-carrying capacity of the pavement layers and ultimately pavement performance. With available climate data from weather stations, the MEPDG uses the Enhanced Integrated Climatic Model (EICM) to predict temperature and moisture within each pavement layer and the subgrade. The temperature and moisture predictions from the EICM are used to estimate material properties for the foundation and pavement layers on a semi-monthly or monthly basis throughout the design life. The frost depth is determined, and the proper moduli are estimated above and below this depth.

For the pavement structure, the surface AC layer is divided into sublayers to account for temperature and aging gradients. Asphalt aging is modeled only for the top sublayer. The largest change in stiffness due to aging occurs only in the top half-inch, and the aging gradient for layers other than the top layer is not significant. The top layer is more susceptible to aging since long-term aging is strongly affected by oxidation. Irrespective of the thickness of the top AC layer, it is always divided in two sublayers (12.7 mm and the remaining thickness). Unbound base layers thicker than 152 mm and unbound subbase layers thicker than 203 mm are divided into sublayers for analysis purposes. For the base layer (first unbound layer), the first sublayer is always 51 mm. The remaining thickness of the base layer and any subbase layers are divided into sublayers with a minimum thickness of 102 mm. For compacted and natural subgrade, the minimum sublayer thickness is 305 mm. A pavement structure is divided into layers only to a depth of 2.4 m. The remaining depth is treated as an infinite layer. If bedrock is present, then the remaining subgrade is treated as one layer beyond 2.4 m; bedrock is not divided into smaller layers and is always treated as an infinite layer.

The material properties of each pavement layer are used to characterize material behavior within the specific response model. Bound materials generally display a linear, or nearly linear, stress-strain relationship. Unbound materials display stress dependent properties. Granular materials are generally “stress hardening” and show an increase in modulus with an increase in stress. Fine-grained soils are generally “stress softening” and display a modulus decrease with increased stress. Material properties associated with pavement distress criteria are normally linked to some measure of material stiffness/strength (dynamic modulus, resilient modulus, and tensile strength).

**Hierarchical Input Level**

One unique feature of the MEPDG is that pavement designers have a great deal of flexibility in obtaining the design input for a design project based on the critical nature of the project and the available resources through the Hierarchical Input Level (HIL). The HIL can be applied to various aspects: traffic, materials, and environmental input. In general, there are three HILs.

Level 1 input results in the highest level of accuracy and, thus, would have the lowest level of uncertainty or error. Input at this level would typically be used for designing heavily trafficked pavement or wherever there are safety concerns or serious economic consequences of early failure. Level 1 material input requires laboratory or field testing, such as the DSR testing of asphalt binder, the complex modulus testing of AC and site-specific axle load spectra. Consequently, obtaining Level 1 input requires more resources and time.

Level 2 input results in an intermediate level of accuracy. This level could be used when resources or testing equipment are not available for tests required for Level 1. Level 2 input typically comes from one of more of three resources: user-selected (possibly from an agency database), derived from a limited testing program, or estimated through correlations. Examples would be estimating the dynamic modulus of AC mixtures from binder, aggregate, and mixture properties or using site-specific traffic volume and traffic classification data in conjunction with agency-specific axle load spectra.

Level 3 input results in the lowest level of accuracy. This level might be used for design where there are minimal consequences of early failure (e.g., lower volume roads). Input typically would be user-selected values or typical averages for the region. Examples include default unbound materials resilient modulus values or default AC mixture properties estimated from aggregate gradation and binder grade.

For the SISSI project, input parameters were obtained using a combination of the three HILs, as given in Table 1.

**Table 1. Available hierarchical input levels of SISSI data.**

| Category | Input | Availability | Hierarchical Input Level |
|---|---|---|---|
| Traffic | Initial AADTT | Y | 1 |
| | Monthly Adjustment Factor | Y | 1 |
| | Vehicle Class Distribution | Y | 1 |
| | Hourly Truck Distribution | Y | 1 |
| | Traffic Growth Factor | N | 3 |
| | Axle Load Distribution Factor | Y | 1 |
| | Lateral Traffic Wander | N | 3 |
| | Number of Axles for Each Vehicle Class | Y | 1 |
| | Axle Configuration | N | 3 |
| | Axle Spacing | Y | 1 |
| | Wheelbase | N | 3 |
| Climate | Weather Data | N | 3 |
| | Ground Water Table Depth | N | 3 |
| Structure | Layer Thickness | Y | 1 |
| Material | AC Mixture | Y | 1 |
| | Binder | Y | 1 |
| | AC General | Y | 1* |
| | PCC | N | 3 |
| | Granular | N | 3 |
| Thermal Cracking | Creep Compliance | N | 3 |
| | Tensile Strength | N | 3 |
| | Coefficient of Thermal Contraction | N | 3 |

* Except for Poisson's ratio, unit weight, and thermal properties

## Performance Models

### Fatigue Cracking

To characterize the fatigue mechanism in AC layers, numerous models can be found in the existing literature. The fatigue-cracking model, which calculates the number of cycles to failure, only expresses the stage of fatigue cracking described as the crack initiation stage. The second stage, or vertical crack propagation stage, is accounted for in these models by using the field adjustment factor. Other models use two different equations to express each stage of the fatigue cracking. For example, Lytton et al. (1993) used fracture mechanics based upon the Paris law to model the crack propagation stage in the development of the theoretical Superpave Model. Finally, a third stage of fatigue fracture is associated with the growth in longitudinal area in which fatigue cracking occurs. In general, true field fatigue failure is associated with a percentage of fatigue cracking along the roadway.

The MEPDG approach first calculates the fatigue damage at critical locations that may be either at the surface and result in longitudinal (top-down) cracking or at the bottom of the AC layer and result in alligator (bottom-up) cracking. The fatigue damage is then correlated using a calibration factor to the fatigue cracking. Estimation of fatigue damage is based upon Miner’s Law, which states that damage is given by the following relationship:

$$D = \sum_{i=1}^{T} \frac{n_i}{N_i} \qquad (1)$$

where $D$ is damage, $T$ is the total number of analysis periods, $n_i$ is actual traffic for analysis period $i$, and $N_i$ is traffic allowed under conditions prevailing in $i$. The relationship used for the prediction of the number of repetitions to fatigue cracking is expressed as:

$$N_f = 0.00432 * k'_1 * (10^{[V_b/(V_a+V_b)-0.69]}) * (\frac{1}{\varepsilon_t})^{3.9492} * (\frac{1}{E})^{1.281} \qquad (2)$$

where $V_b$ is the effective binder content, $V_a$ is the air voids, and $k_1$ is introduced to provide a correction for different asphalt layer thickness ($h_{AC}$) effects. For alligator cracking:

$$k'_1 = \frac{1}{0.000398 + \frac{0.003602}{1 + e^{(11.02 - 3.49 * h_{AC})}}} \qquad (3)$$

For longitudinal cracking:

$$k'_1 = \frac{1}{0.01 + \frac{12.00}{1 + e^{(15.676 - 2.8186 * h_{AC})}}} \qquad (4)$$

In the MEPDG, the mathematical relationship used for fatigue characterization is of the following form. For alligator cracking (percent of total lane area):

$$FC_A = [\frac{6000}{1 + e^{(C_1 + C_2 * \log 10(D * 100))}}] * (\frac{1}{60}) \qquad (5)$$

where $FC_A$ is alligator cracking, percent lane area, $D$ is alligator damage, $C_1$ = -2* $C_2$, $C_2 = -2.40874 - 39.748 * (1 + h_{AC})^{-2.856}$, and $h_{AC}$ is the total thickness of AC layers in inches.

For longitudinal cracking (percent of total lane area):

$$FC_L = [\frac{1000}{1 + e^{(7.0 - 3.5 * \log 10(D * 100))}}] * 10.56 \qquad (6)$$

where $FC_L$ is longitudinal cracking, ft/mile, and $D$ is longitudinal damage. The MEPDG considers that bottom-up fatigue cracking results in “alligator cracking” distress alone, and surface-down fatigue cracking is associated with “longitudinal cracking.”

**Rutting**

Rutting, or permanent deformation, is a load-related distress caused by cumulative applications of loads at moderate to high temperatures when the asphalt concrete mixture has the lowest stiffness. It can be divided into three stages. Primary rutting develops early in the service life and is caused predominantly by densification of the mixture (compaction effort by passing traffic) and with decreasing rate of plastic deformations. In the secondary stage, rutting increments are smaller at a constant rate, and the mixture is mostly undergoing plastic shear deformations. The tertiary stage is when shear failure occurs, and the mixture flows to rupture. In the MEPDG, only rutting in the primary and secondary stages is predicted. Total rutting is the summation of rut depths from all layers, AC, base/subbase, and subgrade.

$$RD_{total} = RD_{AC} + RD_{Base} + RD_{Subgrade} \quad (7)$$

The asphalt concrete layer is sub-divided into sublayers, and the total predicted rut depth for the AC layer is given by:

$$RD_{AC} = \sum_{i=1}^{n} [(\varepsilon_r * k_1 * 10^{-3.4488} T^{1.5606} N^{0.479244})_i * h_{ACi}] \quad (8)$$

where $RD_{AC}$ is rut depth in the AC layer, $n$ is number of sublayers, $\varepsilon_r$ is vertical resilient strain at the middle of the sublayer $i$ for a give load, $k_1$ is depth correction factor, $T$ is temperature, $N$ is number of repetitions for a given load, and $h_{ACi}$ is the thickness of sublayer $i$.

$$k1 = C * 0.328196^{D} \quad (9)$$

where $D$ is depth to the point of strain calculation, and $C$ is calculated as:

$$C = (-0.1039 * h^2{}_{AC} + 2.4868 * h_{AC} - 17.342) + (0.0172 * h^2{}_{AC} - 1.7331 * h_{AC} + 27.428) * D \quad (10)$$

The MEPDG also divides all unbound granular materials into sublayers, and the total rutting for each layer is the summation of the rut depth of all sublayers. The predicted rut depth for the unbound granular base/subbase is as follows:

$$RD_G = \sum_{i=1}^{n} \beta * a * [e^{-(\frac{b}{N})^c}] * \varepsilon_v * h_i \quad (11)$$

where $RD_G$ is rut depth in the unbound granular layer, $\beta$ is calibration factor, $a$, $b$, and $c$ are material properties, $N$ is number of traffic repetitions, and $h_i$ is the thickness of sublayer $i$.

$$\log c = -0.61119 - 0.017638 * W_c \quad (12)$$

$$\log a = \frac{e^{b^c} * 0.15 + e^{(b/10^9)^c}}{2} \quad (13)$$

$$b = 10^9 * (\frac{-4.89285}{1 - 10^{9c}})^{1/c} \quad (14)$$

$$W_c = 51.712 * [(\frac{E_r}{2555})^{1/0.64}]^{-0.3586*GWT^{0.1192}} \tag{15}$$

where $W_c$ is percent water content, $E_r$ is resilient modulus of the unbound granular layer/sublayer in psi, and *GWT* is ground water table depth in ft. The calibration factors, $\beta$, for base/subbase and subgrade are 1.673 and 1.35, respectively.

## Smoothness

The IRI over the pavement life depends on the initial as-constructed longitudinal profile of the pavement from which the initial IRI is computed and on the subsequent incremental development of distresses over time. These distresses include rutting, alligator cracking, longitudinal cracking, and thermal cracking for flexible pavements. In addition, smoothness loss due to soil movements and other climatic factors (depressions, frost heave, and settlement) are considered in the prediction of smoothness through the use of a “site factor” term (represented by a cluster based on foundation and climatic properties). The models for predicting IRI of flexible pavements with a granular base are a function of the base type as described below:

$$IRI = IRI_0 + 0.0463 * [SF * (e^{\frac{age}{20}} - 1)] + 0.00119 * TC_{LT} + 0.1834 * COV_{RD} + 0.00384 * FC_T \tag{16}$$

where *IRI* is *IRI* at any given time, m/km, $IRI_0$ is initial *IRI*, m/km, SF is site factor, $e^{\frac{age}{20}} - 1$ is age term (where age is expressed in years), $COV_{RD}$ is coefficient of variation of the rut depths, percent, $TC_{LT}$ is total length of transverse cracks at all severity levels, m, and $FC_T$ is fatigue cracking (alligator plus longitudinal) in the wheel path, defined as percent of total lane area.

## Running MEPDG Software

Since the MEPDG software (version 0.910) was used as a tool to assess the sensitivity of SISSI site-specific parameters, this section presents details of running the MEPDG software for two of the SISSI sites. A complete input summary for SISS sites at Blair and Warren counties can be found in Appendices A and B, respectively.

## Description of MEPDG Input

A 20-year design life was assumed for both the Warren and Blair sites. Dates of pavement construction and traffic opening were obtained from previous SISSI reports (Solaimanian et al. 2006). Initial IRI values were input as measured during the first profiling activity (Stoffels and Solaimanian 2006). A default reliability level of 90 percent was assumed for all performance criteria. The pavement will have no more than

- an IRI of 2.7 m/km,
- longitudinal cracking of 190 m/km,
- alligator cracking of 25 percent,
- AC thermal fracture (transverse cracking) of 190 m/km, and
- 6.4 mm permanent deformation in the AC layers and 19 mm in the total pavement.

These criteria were kept the same for both Warren and Blair sites. The MEPDG input is grouped under separate modules: traffic, climate, and structure. Some input is highlighted in the following sections.

## Traffic Module

MEPDG-required traffic input was determined from SISSI WIM data. The initial two-way AADTT was 422 and 160 trucks for Warren and Blair, respectively. Truck traffic was assumed equally distributed in both directions (i.e., 50 percent of the trucks drive in the design direction). There were two lanes in the design direction, with 91 percent and 79 percent of the trucks in the design lane for Warren and Blair, respectively. The operational speed was input as 93 and 68 kph for Warren and Blair, respectively. Traffic growth function was determined based on the historical traffic data after the base year: no traffic growth at Warren and a linear growth factor of 8 percent at Blair. Averaged vehicle class and hourly truck distributions were used. By selecting Level 3, the mean of the outer wheel edge was assumed to be located at 0.46 m from the edge of the pavement. The lateral traffic wander has a standard deviation of 0.25 m. The pavement has a standard design lane width of 0.36 m. The number and spacing for each axle type, such as tandem and tridem, was input as Level 1 for each vehicle class. The axle configuration and wheelbase were selected as Level 3 default values.

## Climate Module

There are several methods of inputting climate data into the MEPDG software, depending upon the extent of information available, regardless of the pavement type. The user can either import a previously generated climatic data file or generate one for a specific location. In this study, a new climate data file was generated for each SISSI site. By specifying latitude, longitude, and elevation, the software lists the six closest weather stations in the climate database that are within a radius of 160 km to the site. It also shows the amount of climate data (i.e., 60 months) stored at each weather station. A ground water table depth (*GWT*) of 3 m was assumed, and all six weather stations were selected to interpolate climate data. The software automatically creates a climate data file that contains the sunrise time, sunset time, and radiation for each day of the design life period. In addition, for each 24-hour period in each day of the design life, the temperature, rainfall, air speed, sunshine, and *GWT* are also listed in the climate file. EICM was integrated in the MEPGD software to calculate the pavement temperature for AC materials and moisture content for granular materials.

Researchers (Ongel and Harvey 2004, Yin et al. 2006) reported that the MEPDG software repeats climatic data to fill out the design period. For instance, if the design period is 20 years, but only 5 years of climatic data are available, the MEPDG software determines the temperature profiles for the available 5 years and then reuses the results four times to fill out the design period. In order to isolate the effect introduced by repeating temperature data and avoid any apparent differences that are due to the inclusion of different climatic years, only climate data from the traffic opening date to the most recent available date were utilized. There are 46 and 22 months of climate data for Warren (10/01/2001 to 07/31/2005) and Blair (10/01/2003 to 07/31/2005), respectively. Consequently, only performance measures during these time periods were considered in this sensitivity study.

## Structure Module

The structure module includes structural and material input. The subgrade layer was automatically divided into two sublayers by the software, as required by EICM. The MEPDG software calls for different input for different HILs, as shown in Table 1. For this study, all material properties of AC layers were input as Level 1, while fractured JPCP and granular materials were input as Level 3. For Level 1 AC material properties, the highest temperature for the complex modulus test has to be higher than 52$^{o}$C, and the minimum value of dynamic modulus, $|E^*|$, regardless of temperature and frequency, has to be higher than 69MPa. As presented in the previous report (Solaimanian et al. 2006), 52$^{o}$C was not considered in the complex modulus tests. Therefore, $|E^*|$ values at this temperature were extrapolated from sigmoidal-fitted dynamic modulus master curves. Test frequencies resulting in $|E^*|$ values less than 69 MPa, such as a low frequency at a high temperature, were not used. The structure module also asks the user to provide all input required to predict thermal cracking. The software uses the tensile strength, creep compliance, and coefficient of thermal contraction of AC mixtures to predict thermal cracking. Either the user decides the input values, or the software uses default values that are calculated from the AC material properties entered for the surface layer in the pavement structure. For this part of study, all material properties for thermal cracking prediction were input as Level 3.

## Evaluation of MEPDG Predictions

After all input is provided, the MEPDG software begins the analysis process to predict the performance over the design life of the pavement. At the end of the analysis, the software creates a summary file and other output files. The summary file contains an input summary sheet, computed material modulus values, and distress summaries for all predicted distresses in a tabular format. Further, the predicted distresses and IRI over time are reported. Distresses predicted from the MEPDG software and observed in the field are summarized in Tables 2 and 3 for Blair and Warren sites, respectively. Graphic representations are also provided in Figures 2 through 7. The following observations can be made based on the results presented in these tables and figures.

- The MEPDG software did not predict any longitudinal (top-down) cracking for both Blair and Warren sites.
- Total rut depth predicted from the MEPDG software displays a good agreement with field observations. Excessive rutting occurred in unbound layers during the first few months after the section was opened to traffic. This phenomenon may have resulted from a combined effect of the initial traffic compaction and the low values of backcalculated resilient moduli of granular layers in the summer.
- During the time frame between the two pavement condition surveys at the Blair site, a significant increase in rut depth was shown to occur based on MEPDG predictions, while no such increase was observed in the field. Similar divergence was observed in alligator cracking at both Blair and Warren sites. These differences may arise from the measurement error of manual distress survey and from transverse profiling.
- A closer agreement between predictions and field conditions was observed for smoothness.

**Table 2. Comparison of performance predictions and field conditions for Blair.**

| Distress | | Sep-04 | Dec-05 |
|---|---|---|---|
| Alligator Cracking, % | MEPDG | 0.0 | 0.4 |
| | Field | 0.0 | 1.4 |
| Longitudinal Cracking, m/km | MEPDG | 0.0 | 0.0 |
| | Field | 0.0 | 0.0 |
| Rut Depth, mm | MEPDG, AC | 5.4 | 6.3 |
| | MEPDG, Granular | 5.4 | 6.3 |
| | MEPDG, Total | 5.4 | 6.3 |
| | Field, LWP | 2.8 | 3.5 |
| | Field, RWP | 2.6 | 4.3 |
| IRI, m/km | MEPDG | 1.323 | 1.362 |
| | Field | 1.444 | 1.397 |

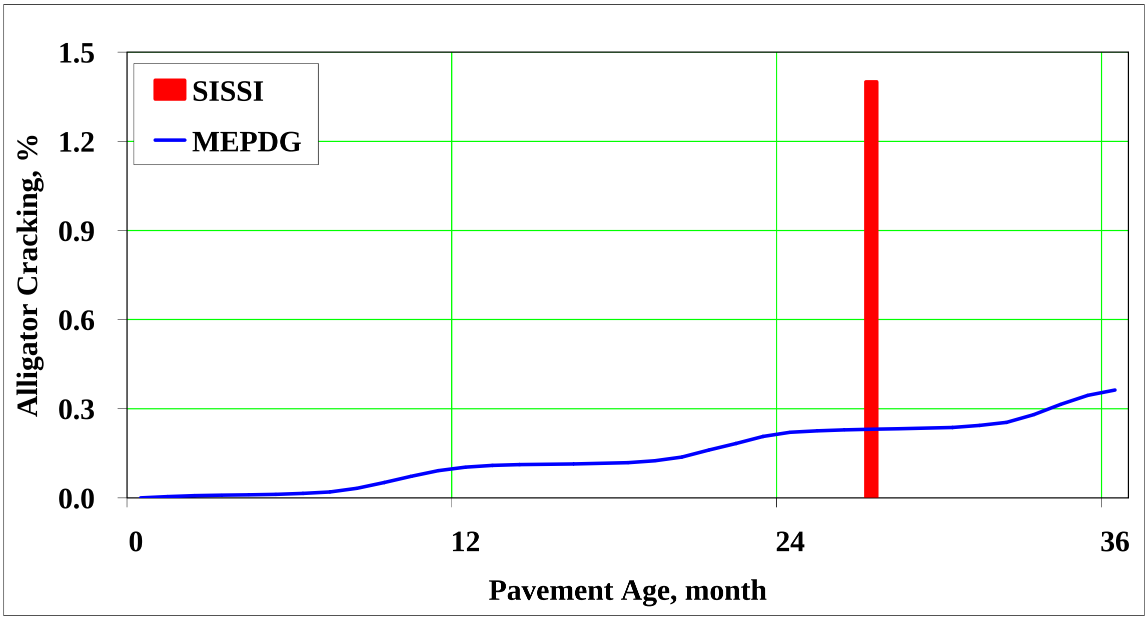


**Figure 1. Alligator cracking predictions vs. field measurements for Blair**

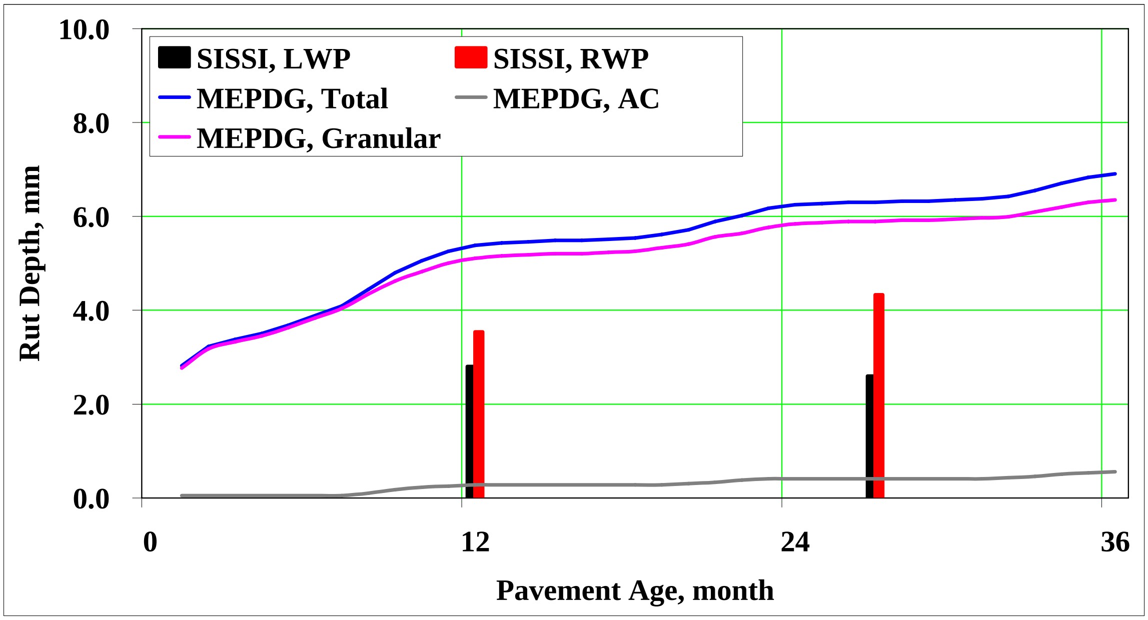


**Figure 2. Rutting predictions vs. field measurements for Blair**

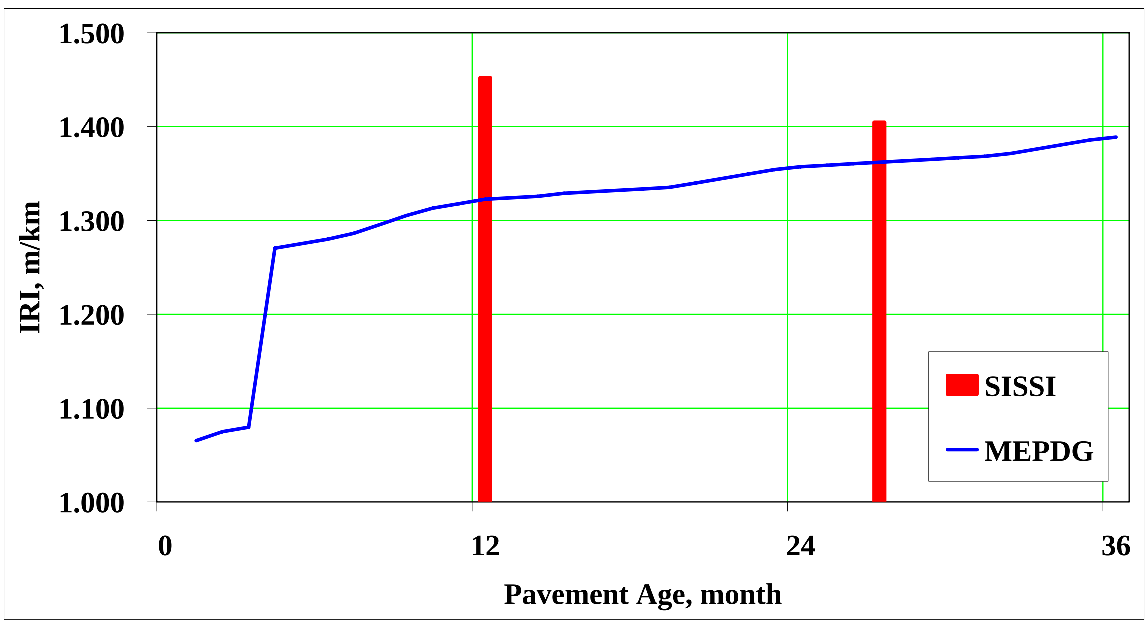


**Figure 3. Smoothness predictions vs. field measurements for Blair**

**Table 3. Comparison of performance predictions and field conditions for Warren.**

| Distress | | Mar-04 | Dec-04 | Feb-05 | Jun-05 |
|---|---|---|---|---|---|
| Alligator | MEPDG | 0.0 | 0.0 | 0.0 | 0.0 |

| | | | | | |
|---|---|---|---|---|---|
| | Field | - | 0.2 | - | 2.3 |
| Longitudinal Cracking, m/km | MEPDG | 0.0 | 0.0 | 0.0 | 0.0 |
| | Field | - | 0.0 | - | 67.7 |
| Rut Depth, mm | MEPDG, AC | 0.4 | 0.5 | 0.5 | 0.5 |
| | MEPDG, Granular | 5.2 | 5.7 | 5.7 | 5.8 |
| | MEPDG, Total | 5.6 | 6.2 | 6.2 | 6.3 |
| | Field, LWP | 7.4 | - | 7.3 | - |
| | Field, RWP | 7.4 | - | 7.3 | - |
| IRI, m/km | MEPDG | 0.873 | 0.898 | 0.899 | 0.909 |
| | Field | - | 0.773 | - | 0.868 |

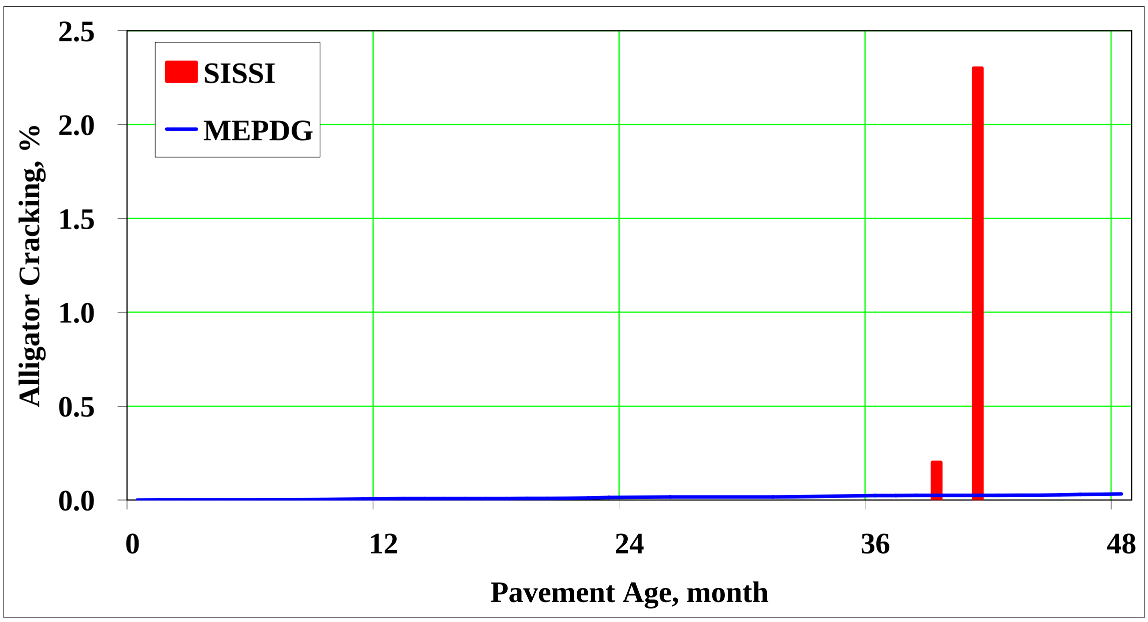


**Figure 4. Alligator cracking predictions vs. field measurements for Warren**

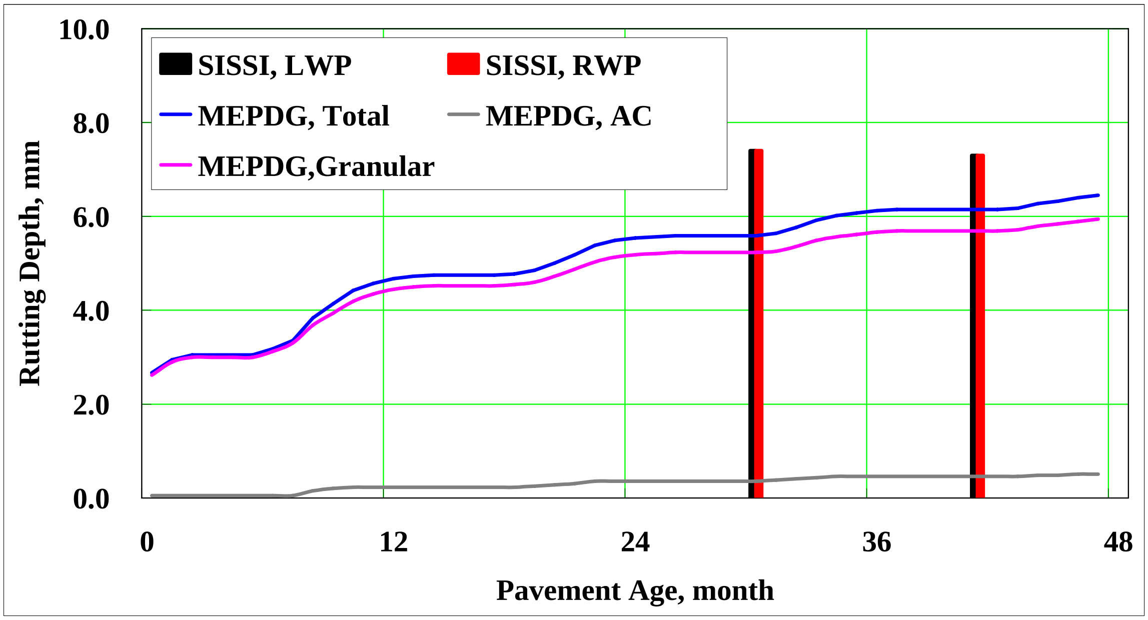


Figure 5. Rutting predictions vs. field measurement for Warren

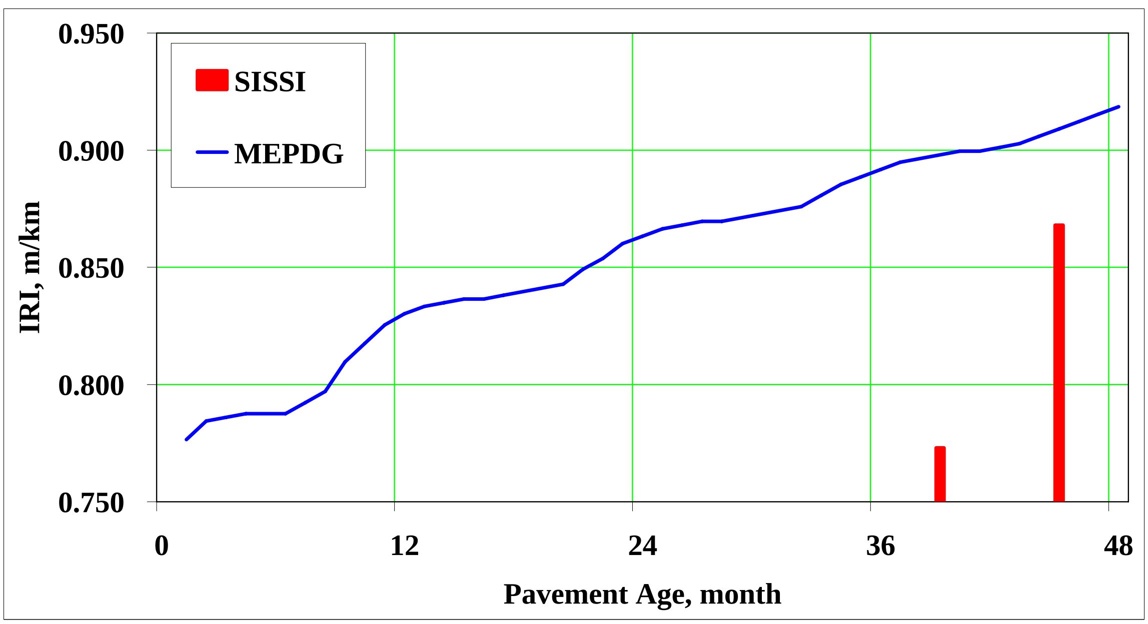


Figure 6. Smoothness predictions vs. field measurement for Warren

**Summary**

This report presents performance predictions for two SISSI sites using the MEPDG software. Details on running the MEPDG software are also provided. Predicted pavement performance was evaluated using available field measured data for both Blair and Warren sites. Overall, for most cases, the MEPDG software results are significantly different from measured values. The discrepancy observed between the predictions and field conditions is perhaps due to the national calibration coefficients in the empirical performance models. This difference indicates that local calibration of the MEPDG software is crucial to obtain reliable results. . It is believed that with the availability of large amounts of field condition data, the MEPDG models could be more accurately calibrated locally. Thermal cracking was not considered in the data presented here. Consequently, the contribution of alligator cracking and rutting to IRI may possibly be overestimated

**References**

ERES Consultants Division. (2004) *Guide for Mechanistic-Empirical Design of New and Rehabilitated Pavement Structures*. Final Report NCHRP 1-37A, Champaign, IL.

Lytton, L.R., Uzan, J., Fernando, E. G., Roque, R., Hiltunen, D., and Stoffels, S.M. (1993) *Development and Validation of Performance Prediction Models and Specifications for Asphalt Binders and Paving Mixes*. SHRP-A-357 Report. Strategic Highway Research Program, National Research Council, Washington, D.C.

Newcomb, D.E., Bu-bushait, A.A., Mahoney, J.P. and Sharma, J. (1983) *State-of-the-Art on Pavement Overlay Design Procedures*. *Vol. 1*. Report No. WA-RD 65.1, Washington State Department of Transportation, Olympia, WA.

Ongel, A. and Harvey, J. (2004) *Analysis of 30 Years of Pavement Temperatures using the Enhanced Integrated Climate Model (EICM)*. Draft report prepared for the California Department of Transportation, Pavement Research Center, Institute of Transportation Studies, University of California, Berkeley, University of California, Davis, CA.

Solaimanian, M., Hunter, D., and Stoffels, S. M. (2006) *Design and Construction Report for Superpave In-Situ Stress-Strain Instrumentation Sites, State Route 1001, Blair County, Pennsylvania*. Final Report, Pennsylvania Transportation Institute, University Park, PA.

Solaimanian, M., Stoffels, S. M., Anderson, D. A., and Morian, D. (2006) *Design and Construction Report for Superpave In-Situ Stress-Strain Instrumentation Sites, State Route 0006, Warren County, Pennsylvania*. Final Report, Pennsylvania Transportation Institute, University Park, PA.

Solaimanian M., Hunter, D. A., Shah, J., and Stoffels, S. M. (2006) *Characterization of Materials for Superpave In-Situ Stress/Strain Investigation*. Final Report, Pennsylvania Transportation Institute, University Park, PA.

Stoffels, S. M. and Solaimanian M. (2006) *Pavement Condition for Superpave In-Situ Stress/Strain Investigation*. Final Report, Pennsylvania Transportation Institute, University Park, PA.

Timm, D.H. and Newcomb, D.E. (2003) “Calibration of Flexible Pavement Performance Equations.” *Transportation Research Record 1853*, Transportation Research Board, Washington, D.C.

Yin, H., Chehab, G., and Stoffels, S. (2006) “Sensitivity of Thermal Cracking Prediction to AC Mixture Properties Using the M-E Pavement Design Guide.” Presented at the 10th International Conference on Asphalt Pavements, Quebec, Canada.

# Appendix A: MEPDG Input Summary for Blair

## General Information

| | |
|---|---|
| Design Life | 20 years |
| Base/Subgrade construction: | August, 2003 |
| Pavement construction: | September, 2003 |
| Traffic open: | October, 2003 |
| Type of design | Flexible |

## Performance Criteria

| | Limit | Reliability |
|---|---|---|
| Initial IRI (in/mi) | 80 | |
| Terminal IRI (in/mi) | 172 | 90 |
| AC Surface Down Cracking (Long. Cracking) (ft/mile): | 1000 | 90 |
| AC Bottom Up Cracking (Alligator Cracking) (%): | 25 | 90 |
| AC Thermal Fracture (Transverse Cracking) (ft/mi): | 1000 | 90 |
| Chemically Stabilized Layer (Fatigue Fracture) | 25 | 90 |
| Permanent Deformation (AC Only) (in): | 0.25 | 90 |
| Permanent Deformation (Total Pavement) (in): | 0.75 | 90 |

| | |
|---|---|
| Location: | Blair County, PA |
| Project ID: | State Rute 1001 |
| Section ID: | 0030-0031 |
| Traffic direction: | South bound |

## Traffic

| | |
|---|---|
| Initial two-way aadtt: | 160 |
| Number of lanes in design direction: | 2 |
| Percent of trucks in design direction (%): | 48.5 |
| Percent of trucks in design lane (%): | 79.1 |
| Operational speed (mph): | 42.5 |

## Traffic -- Volume Adjustment Factors

**Monthly Adjustment Factors** (Level 1, Site Specific - MAF)

| | Vehicle Class | | | | | | | | | |
|---|---|---|---|---|---|---|---|---|---|---|
| Month | Class 4 | Class 5 | Class 6 | Class 7 | Class 8 | Class 9 | Class 10 | Class 11 | Class 12 | Class 13 |
| January | 1.18 | 1.26 | 0.93 | 0.44 | 0.71 | 0.92 | 0.67 | 0.00 | 0.28 | 2.24 |
| February | 1.23 | 1.23 | 0.99 | 0.61 | 0.94 | 0.95 | 0.89 | 1.30 | 1.93 | 0.00 |
| March | 1.19 | 1.21 | 0.94 | 1.11 | 0.92 | 0.94 | 0.84 | 1.23 | 2.64 | 0.00 |
| April | 1.16 | 1.26 | 1.08 | 1.29 | 1.10 | 1.01 | 1.56 | 2.78 | 0.50 | 0.00 |
| May | 1.19 | 1.27 | 1.13 | 1.85 | 1.09 | 0.91 | 1.94 | 0.32 | 1.38 | 1.68 |
| June | 0.53 | 1.11 | 1.13 | 1.92 | 1.16 | 1.09 | 1.79 | 1.27 | 0.50 | 0.00 |
| July | 0.28 | 1.00 | 1.23 | 1.01 | 1.08 | 0.98 | 0.77 | 0.00 | 0.22 | 0.00 |
| August | 0.45 | 1.10 | 0.99 | 1.00 | 1.10 | 1.01 | 0.76 | 1.42 | 2.92 | 1.35 |
| September | 1.30 | 1.24 | 0.99 | 1.21 | 1.14 | 1.02 | 0.81 | 1.30 | 1.38 | 3.36 |
| October | 1.27 | 1.31 | 1.00 | 0.71 | 1.03 | 1.19 | 0.64 | 0.43 | 0.00 | 0.00 |
| November | 1.13 | 0.00 | 0.81 | 0.55 | 0.92 | 1.05 | 1.04 | 1.30 | 0.00 | 0.00 |
| December | 1.11 | 0.00 | 0.78 | 0.31 | 0.79 | 0.92 | 0.30 | 0.65 | 0.28 | 3.36 |

**Vehicle Class Distribution**

(Level 1, Site Specific Distribution )

**AADTT distribution by vehicle class**

| | |
|---|---|
| Class 4 | 6.6% |
| Class 5 | 34.5% |
| Class 6 | 12.7% |
| Class 7 | 2.1% |
| Class 8 | 18.3% |
| Class 9 | 25.0% |
| Class 10 | 0.5% |
| Class 11 | 0.1% |
| Class 12 | 0.1% |
| Class 13 | 0.1% |

**Hourly truck traffic distribution**

by period beginning:

| | | | |
|---|---|---|---|
| Midnight | 1.7% | Noon | 5.9% |
| 1:00 am | 1.9% | 1:00 pm | 6.3% |
| 2:00 am | 1.9% | 2:00 pm | 7.0% |
| 3:00 am | 1.7% | 3:00 pm | 4.9% |
| 4:00 am | 5.5% | 4:00 pm | 3.8% |
| 5:00 am | 3.9% | 5:00 pm | 3.6% |
| 6:00 am | 5.4% | 6:00 pm | 3.2% |
| 7:00 am | 7.4% | 7:00 pm | 1.7% |
| 8:00 am | 7.7% | 8:00 pm | 1.6% |
| 9:00 am | 7.6% | 9:00 pm | 1.0% |
| 10:00 am | 7.8% | 10:00 pm | 1.1% |
| 11:00 am | 6.3% | 11:00 pm | 1.2% |

**Traffic Growth Factor**

| Vehicle Class | Growth Rate | Growth Function |
|---|---|---|
| Class 4 | 8.0% | Linear |
| Class 5 | 8.0% | Linear |
| Class 6 | 8.0% | Linear |
| Class 7 | 8.0% | Linear |
| Class 8 | 8.0% | Linear |
| Class 9 | 8.0% | Linear |
| Class 10 | 8.0% | Linear |
| Class 11 | 8.0% | Linear |
| Class 12 | 8.0% | Linear |
| Class 13 | 8.0% | Linear |

## Traffic -- Axle Load Distribution Factors

Level 1: Site Specific

## Traffic -- General Traffic Inputs

| | |
|---|---|
| Mean wheel location (inches from the lane marking): | 18 |
| Traffic wander standard deviation (in): | 10 |
| Design lane width (ft): | 12 |

**Number of Axles per Truck**

| Vehicle Class | Single Axle | Tandem Axle | Tridem Axle | Quad Axle |
|---|---|---|---|---|
| Class 4 | 1.83 | 0.17 | 0.00 | 0.00 |
| Class 5 | 2.00 | 0.00 | 0.00 | 0.00 |
| Class 6 | 1.00 | 1.00 | 0.00 | 0.00 |
| Class 7 | 1.03 | 0.03 | 0.97 | 0.00 |
| Class 8 | 2.41 | 0.59 | 0.00 | 0.00 |
| Class 9 | 1.11 | 1.95 | 0.00 | 0.00 |
| Class 10 | 1.00 | 1.00 | 1.00 | 0.00 |
| Class 11 | 5.00 | 0.00 | 0.00 | 0.00 |
| Class 12 | 4.00 | 1.00 | 0.00 | 0.00 |
| Class 13 | 1.70 | 1.10 | 0.50 | 0.40 |

## Axle Configuration

| | |
|---|---|
| Average axle width (edge-to-edge) outside dimensions,ft): | 8.5 |
| Dual tire spacing (in): | 12 |

**Axle Configuration**

| | |
|---|---|
| Tire Pressure (psi) : | 120 |

**Average Axle Spacing**

| | |
|---|---|
| Tandem axle(psi): | 50.86 |
| Tridem axle(psi): | 54.63 |
| Quad axle(psi): | 0 |

## Climate

| | |
|---|---|
| icm file: | Blair |
| Latitude (degrees.minutes) | 40.26 |
| Longitude (degrees.minutes) | -78.25 |
| Elevation (ft) | 1500 |
| Depth of water table (ft) | 10 |

## Structure--Design Features

## Structure--Layers

### Layer 1 -- Asphalt concrete

Material type: Asphalt concrete
Layer thickness (in): 2.1

**General Properties**

General
Reference temperature (F°): 77

Volumetric Properties as Built
Effective binder content (%): 10.3
Air voids (%): 7.7
Total unit weight (pcf): 164

Poisson's ratio: 0.35 (user entered)

Thermal Properties
Thermal conductivity asphalt (BTU/hr-ft-F°): 0.67
Heat capacity asphalt (BTU/lb-F°): 0.23

**Asphalt Mix**

Number of temperatures: 5
Number of frequencies: 6

| Temperature °F | Mixture E* (psi) | | | | | |
|---|---|---|---|---|---|---|
| | 0.1 | 0.5 | 1 | 5 | 10 | 25 |
| 39 | 1347939 | 1742175 | 1908239 | 2313528 | 2551768 | 2795984 |
| 50 | 857027 | 1226019 | 1378936 | 1775424 | 1958385 | 2212632 |
| 77 | 198104 | 370422 | 451182 | 706600 | 840894 | 1042792 |
| 104 | 41025 | 77507 | 103356 | 206528 | 271232 | 379020 |
| 127 | 16206 | 40210 | 57144 | 118877 | 157662 | 222695 |

**Asphalt Binder**

Option: Superpave binder test data

| Temperature °F | Angular frequency = 10 rad/sec | |
|---|---|---|
| | G*, psi | Delta (°) |
| 126 | 35216 | 77 |
| 136 | 15336 | 81 |
| 147 | 6673 | 83 |
| 158 | 3271 | 85 |
| 169 | 1492 | 87 |

### Layer 2 -- Asphalt concrete

Material type: Asphalt concrete
Layer thickness (in): 1.9

**General Properties**

General
Reference temperature (F°): 77

Volumetric Properties as Built
Effective binder content (%): 9.5
Air voids (%): 6.4
Total unit weight (pcf): 164

Poisson's ratio: 0.35 (user entered)

Thermal Properties
Thermal conductivity asphalt (BTU/hr-ft-F°): 0.67
Heat capacity asphalt (BTU/lb-F°): 0.23

**Layer 4 -- A-2-7**

| | |
|---|---|
| Unbound Material: | A-2-7 |
| Thickness(in): | 8 |

**Strength Properties**

| | |
|---|---|
| Input Level: | Level 3 |
| Analysis Type: | ICM inputs (ICM Calculated Modulus) |
| Poisson's ratio: | 0.35 |
| Coefficient of lateral pressure,Ko: | 0.5 |
| Modulus (input) (psi): | 17000 |

**ICM Inputs**

Gradation and Plasticity Index

| | |
|---|---|
| Plasticity Index, PI: | 12 |
| Liquid Limit (LL) | 45 |
| Compacted Layer | No |
| Passing #200 sieve (%): | 5 |
| Passing #40 | 14.4 |
| Passing #4 sieve (%): | 37 |
| D10(mm) | 0.1879 |
| D20(mm) | 1.18 |
| D30(mm) | 2.677 |
| D60(mm) | 11.73 |
| D90(mm) | 33.41 |

| Sieve | Percent Passing |
|---|---|
| **0.001mm** | |
| **0.002mm** | |
| **0.020mm** | |
| **#200** | 5 |
| **#100** | |
| **#80** | |
| **#60** | |
| **#50** | |
| **#40** | |
| **#30** | |
| **#20** | |
| **#16** | 20 |
| **#10** | |
| **#8** | |
| **#4** | 37 |
| **3/8"** | 53 |
| **1/2"** | |
| **3/4"** | 76 |
| **1"** | |
| **1 1/2"** | |
| **2"** | 100 |
| **2 1/2"** | |
| **3"** | |
| **3 1/2"** | |
| **4"** | |

Calculated/Derived Parameters

| | |
|---|---|
| Maximum dry unit weight (pcf): | 127.0 (derived) |
| Specific gravity of solids, Gs: | 2.70 (derived) |
| Saturated hydraulic conductivity (ft/hr): | 0.06599 (derived) |
| Optimum gravimetric water content (%): | 7.5 (derived) |
| Calculated degree of saturation (%): | 61.8 (calculated) |

Soil water characteristic curve parameters: Default values

| Parameters | Value |
|---|---|
| **a** | 5.9544 |
| **b** | 1.932 |
| **c** | 0.79215 |
| **Hr.** | 220 |

**Layer 5 -- A-2-7**

| | |
|---|---|
| Unbound Material: | A-2-7 |
| Thickness(in): | 10 |

**Strength Properties**

| | |
|---|---|
| Input Level: | Level 3 |
| Analysis Type: | ICM inputs (ICM Calculated Modulus) |
| Poisson's ratio: | 0.35 |
| Coefficient of lateral pressure,Ko: | 0.5 |
| Modulus (input) (psi): | 17000 |

**ICM Inputs**

Gradation and Plasticity Index

| | |
|---|---|
| Plasticity Index, PI: | 12 |
| Liquid Limit (LL) | 45 |
| Compacted Layer | No |
| Passing #200 sieve (%): | 27.4 |
| Passing #40 | 37.1 |
| Passing #4 sieve (%): | 55.4 |
| D10(mm) | 0.00112 |
| D20(mm) | 0.01255 |
| D30(mm) | 0.1349 |
| D60(mm) | 5.73 |
| D90(mm) | 26.71 |

| Sieve | Percent Passing |
|---|---|
| 0.001mm | |
| 0.002mm | |
| 0.020mm | |
| #200 | 27.4 |
| #100 | |
| #80 | 32 |
| #60 | |
| #50 | |
| #40 | 37.1 |
| #30 | |
| #20 | |
| #16 | |
| #10 | 47.6 |
| #8 | |
| #4 | 55.4 |
| 3/8" | 72.4 |
| 1/2" | 78.1 |
| 3/4" | 85.3 |
| 1" | 89.1 |
| 1 1/2" | 94.6 |
| 2" | 97 |
| 2 1/2" | |
| 3" | |
| 3 1/2" | 100 |
| 4" | 100 |

Calculated/Derived Parameters

| | |
|---|---|
| Maximum dry unit weight (pcf): | 120.8 (derived) |
| Specific gravity of solids, Gs: | 2.70 (derived) |
| Saturated hydraulic conductivity (ft/hr): | 1.868e-006 (derived) |
| Optimum gravimetric water content (%): | 10.6 (derived) |
| Calculated degree of saturation (%): | 72.4 (calculated) |

Soil water characteristic curve parameters: Default values

| Parameters | Value |
|---|---|
| a | 71.521 |
| b | 0.97264 |
| c | 0.45811 |
| Hr. | 500 |

## Appendix B: MEPDG Input Summary for Warren

## General Information

| | |
|---|---|
| Design Life | 20 years |
| Pavement overlay construction: | September, 2001 |
| Traffic open: | October, 2001 |
| Type of design | Flexible |

## Performance Criteria

| | Limit | Reliability |
|---|---|---|
| Initial IRI (in/mi) | 45 | |
| Terminal IRI (in/mi) | 172 | 90 |
| AC Surface Down Cracking (Long. Cracking) (ft/mile): | 1000 | 90 |
| AC Bottom Up Cracking (Alligator Cracking) (%): | 25 | 90 |
| AC Thermal Fracture (Transverse Cracking) (ft/mi): | 1000 | 90 |
| Permanent Deformation (AC Only) (in): | 0.25 | 90 |
| Permanent Deformation (Total Pavement) (in): | 0.75 | 90 |

| | |
|---|---|
| Location: | Starbrick, Warren County, PA |
| Project ID: | SR 0006 |
| Section ID: | Segment 420 |
| Traffic direction: | East bound |

## Traffic

| | |
|---|---|
| Initial two-way aadtt: | 422 |
| Number of lanes in design direction: | 2 |
| Percent of trucks in design direction (%): | 50 |
| Percent of trucks in design lane (%): | 90.5 |
| Operational speed (mph): | 58 |

## Traffic -- Volume Adjustment Factors

**Monthly Adjustment Factors** (Level 1, Site Specific - MAF)

| | Vehicle Class | | | | | | | | | |
|---|---|---|---|---|---|---|---|---|---|---|
| **Month** | **Class 4** | **Class 5** | **Class 6** | **Class 7** | **Class 8** | **Class 9** | **Class 10** | **Class 11** | **Class 12** | **Class 13** |
| January | 1.12 | 0.48 | 0.74 | 0.36 | 0.93 | 0.88 | 0.46 | 0.34 | 1.41 | 0.35 |
| February | 1.04 | 0.54 | 0.88 | 0.68 | 0.90 | 0.91 | 0.62 | 0.46 | 1.76 | 0.35 |
| March | 0.87 | 0.90 | 0.82 | 0.55 | 0.93 | 0.95 | 0.85 | 0.69 | 0.00 | 0.84 |
| April | 1.18 | 1.04 | 0.84 | 0.91 | 1.09 | 1.03 | 0.75 | 1.40 | 0.00 | 1.33 |
| May | 1.27 | 1.25 | 1.13 | 1.13 | 0.98 | 1.07 | 0.91 | 1.01 | 0.00 | 1.40 |
| June | 0.83 | 1.29 | 1.15 | 1.52 | 1.04 | 1.09 | 1.01 | 1.84 | 0.00 | 0.98 |
| July | 0.63 | 1.18 | 1.16 | 1.11 | 1.07 | 1.06 | 0.95 | 0.71 | 0.00 | 1.33 |
| August | 0.82 | 1.19 | 1.31 | 1.07 | 1.12 | 1.11 | 1.01 | 0.47 | 7.06 | 1.28 |
| September | 1.38 | 1.14 | 1.36 | 1.21 | 1.08 | 1.03 | 1.55 | 1.45 | 0.00 | 0.98 |
| October | 1.14 | 1.16 | 1.08 | 1.59 | 1.02 | 1.08 | 1.48 | 1.45 | 1.76 | 1.61 |
| November | 0.89 | 0.94 | 0.82 | 1.01 | 0.94 | 0.94 | 1.08 | 0.53 | 0.00 | 0.00 |
| December | 0.84 | 0.89 | 0.71 | 0.86 | 0.91 | 0.83 | 1.32 | 1.65 | 0.00 | 1.54 |

**Vehicle Class Distribution**

(Level 1, Site Specific Distribution )

**AADTT distribution by vehicle class**

| | |
|---|---|
| Class 4 | 1.7% |
| Class 5 | 22.5% |
| Class 6 | 12.5% |
| Class 7 | 6.7% |
| Class 8 | 2.7% |
| Class 9 | 52.9% |
| Class 10 | 0.9% |
| Class 11 | 0.1% |
| Class 12 | 0.0% |
| Class 13 | 0.0% |

**Hourly truck traffic distribution**

by period beginning:

| | | | |
|---|---|---|---|
| Midnight | 1.3% | Noon | 6.5% |
| 1:00 am | 1.5% | 1:00 pm | 6.1% |
| 2:00 am | 2.0% | 2:00 pm | 6.0% |
| 3:00 am | 2.9% | 3:00 pm | 5.4% |
| 4:00 am | 3.6% | 4:00 pm | 4.6% |
| 5:00 am | 4.0% | 5:00 pm | 3.5% |
| 6:00 am | 5.4% | 6:00 pm | 2.9% |
| 7:00 am | 6.7% | 7:00 pm | 2.4% |
| 8:00 am | 7.2% | 8:00 pm | 2.1% |
| 9:00 am | 7.1% | 9:00 pm | 1.8% |
| 10:00 am | 7.0% | 10:00 pm | 1.7% |
| 11:00 am | 6.9% | 11:00 pm | 1.4% |

**Traffic Growth Factor**

| Vehicle Class | Growth Rate | Growth Function |
|---|---|---|
| Class 4 | 4.0% | No Growth |
| Class 5 | 4.0% | No Growth |
| Class 6 | 4.0% | No Growth |
| Class 7 | 4.0% | No Growth |
| Class 8 | 4.0% | No Growth |
| Class 9 | 4.0% | No Growth |
| Class 10 | 4.0% | No Growth |
| Class 11 | 4.0% | No Growth |
| Class 12 | 4.0% | No Growth |
| Class 13 | 4.0% | No Growth |

## Traffic -- Axle Load Distribution Factors

Level 1: Site Specific

## Traffic -- General Traffic Inputs

| | |
|---|---|
| Mean wheel location (inches from the lane marking): | 18 |
| Traffic wander standard deviation (in): | 10 |
| Design lane width (ft): | 12 |

**Number of Axles per Truck**

| Vehicle Class | Single Axle | Tandem Axle | Tridem Axle | Quad Axle |
|---|---|---|---|---|
| Class 4 | 1.85 | 0.15 | 0.00 | 0.00 |
| Class 5 | 2.00 | 0.01 | 0.00 | 0.00 |
| Class 6 | 1.00 | 1.00 | 0.00 | 0.00 |
| Class 7 | 1.00 | 0.00 | 1.00 | 0.00 |
| Class 8 | 2.31 | 0.69 | 0.00 | 0.00 |
| Class 9 | 1.22 | 1.89 | 0.00 | 0.00 |
| Class 10 | 1.02 | 1.00 | 0.99 | 0.00 |
| Class 11 | 5.00 | 0.00 | 0.00 | 0.00 |
| Class 12 | 4.00 | 1.00 | 0.00 | 0.00 |
| Class 13 | 1.21 | 0.88 | 0.94 | 0.33 |

## Axle Configuration

| | |
|---|---|
| Average axle width (edge-to-edge) outside dimensions,ft): | 8.5 |
| Dual tire spacing (in): | 12 |

**Axle Configuration**

| | |
|---|---|
| Tire Pressure (psi) : | 120 |

**Average Axle Spacing**

| | |
|---|---|
| Tandem axle(psi): | 50.6 |
| Tridem axle(psi): | 54.1 |
| Quad axle(psi): | 48.1 |

## Climate

| | |
|---|---|
| icm file: | C:\DG2002\Projects\Warren\Warren.icm |
| Latitude (degrees.minutes) | 41.51 |
| Longitude (degrees.minutes) | -79.18 |
| Elevation (ft) | 1259 |
| Depth of water table (ft) | 10 |

## Structure--Design Features

## Structure--Layers

### Layer 1 -- Asphalt concrete

Material type: Asphalt concrete
Layer thickness (in): 1.5

**General Properties**

General
Reference temperature (F°): 77

Volumetric Properties as Built
Effective binder content (%): 12.7
Air voids (%): 6.4
Total unit weight (pcf): 137

Poisson's ratio: 0.35 (user entered)

Thermal Properties
Thermal conductivity asphalt (BTU/hr-ft-F°): 0.67
Heat capacity asphalt (BTU/lb-F°): 0.23

**Asphalt Mix**

Number of temperatures: 5
Number of frequencies: 5

| Temperature °F | Mixture E* (psi) | | | | |
|---|---|---|---|---|---|
| | 0.5 | 1 | 5 | 10 | 25 |
| 39.2 | 1319287 | 1540373 | 1868956 | 2016895 | 2251469 |
| 50 | 794594 | 940212 | 1217930 | 1343920 | 1531308 |
| 77 | 227071 | 293837 | 487569 | 588660 | 740563 |
| 104 | 32914 | 60302 | 123379 | 165778 | 248740 |
| 127.4 | 15264 | 23773 | 59008 | 83291 | 126335 |

**Asphalt Binder**

Option: Superpave binder test data

| Temperature °F | Angular frequency = 10 rad/sec | |
|---|---|---|
| | G*, psi | Delta (°) |
| 114.8 | 33601 | 76 |
| 125.6 | 14109 | 79 |
| 136.4 | 6241 | 82 |
| 147.2 | 2861 | 84 |
| 158 | 1371 | 86 |
| 167 | 699 | 88 |
| 177.8 | 370 | 89 |

### Layer 2 -- Asphalt concrete

Material type: Asphalt concrete
Layer thickness (in): 2.5

**General Properties**

General
Reference temperature (F°): 77

Volumetric Properties as Built
Effective binder content (%): 9.3
Air voids (%): 5.7
Total unit weight (pcf): 142

Poisson's ratio: 0.35 (user entered)

Thermal Properties
Thermal conductivity asphalt (BTU/hr-ft-F°): 0.67
Heat capacity asphalt (BTU/lb-F°): 0.23

**Asphalt Mix**
Number of temperatures: 5
Number of frequencies: 6

| Temperature | Mixture E* (psi) | | | | | |
|---|---|---|---|---|---|---|
| °F | 0.1 | 0.5 | 1 | 5 | 10 | 25 |
| **39.2** | 1289966 | 1465848 | 1691053 | 1944956 | 2086126 | 2290194 |
| **50** | 910305 | 1138609 | 1325340 | 1610934 | 1740211 | 1947905 |
| **77** | 289350 | 472997 | 575698 | 831260 | 958603 | 1151165 |
| **104** | 58837 | 114904 | 160528 | 304144 | 385075 | 523925 |
| **127.4** | 20870 | 55428 | 79864 | 166782 | 219385 | 304343 |

**Asphalt Binder**
Option: Superpave binder test data

| Temperature | Angular frequency = 10 rad/sec | |
|---|---|---|
| °F | G*, psi | Delta (°) |
| **114.8** | 42069 | 75 |
| **125.6** | 17537 | 78 |
| **136.4** | 7754 | 81 |
| **147.2** | 3481 | 83 |
| **156.2** | 1646 | 86 |
| **167** | 815 | 87 |
| **177.8** | 425 | 88 |

## Layer 3 -- Asphalt concrete

Material type: Asphalt concrete
Layer thickness (in): 5.5

**General Properties**
General
Reference temperature (F°): 77

Volumetric Properties as Built
Effective binder content (%): 8.1
Air voids (%): 6.7
Total unit weight (pcf): 147.5

Poisson's ratio: 0.35 (user entered)

Thermal Properties
Thermal conductivity asphalt (BTU/hr-ft-F°): 0.67
Heat capacity asphalt (BTU/lb-F°): 0.23

**Asphalt Mix**
Number of temperatures: 5
Number of frequencies: 6

| Temperature | Mixture E* (psi) | | | | | |
|---|---|---|---|---|---|---|
| °F | 0.1 | 0.5 | 1 | 5 | 10 | 25 |
| **39.2** | 1446703 | 1669201 | 1868125 | 2171167 | 2299912 | 2462257 |
| **50** | 1003516 | 1275583 | 1483011 | 1801804 | 1946551 | 2141386 |
| **77** | 276152 | 507763 | 608989 | 902473 | 1049831 | 1259459 |
| **104** | 48394 | 101613 | 147827 | 301388 | 388749 | 532288 |
| **127.4** | 14974 | 45682 | 69019 | 157194 | 212811 | 304654 |

**Asphalt Binder**

Option: Superpave binder test data

| Temperature °F | Angular frequency = 10 rad/sec | |
|---|---|---|
| | G*, psi | Delta (°) |
| **114.8** | 37571 | 75 |
| **125.6** | 15826 | 79 |
| **136.4** | 6994 | 81 |
| **147.2** | 3180 | 84 |
| **158** | 1496 | 86 |
| **167** | 756 | 87 |
| **177.8** | 397 | 89 |

## Layer 4 -- Asphalt concrete

Material type: Asphalt concrete
Layer thickness (in): 4.4

**General Properties**

General
Reference temperature (F°): 77

Volumetric Properties as Built
Effective binder content (%): 9.3
Air voids (%): 5.7
Total unit weight (pcf): 142

Poisson's ratio: 0.35 (user entered)

Thermal Properties
Thermal conductivity asphalt (BTU/hr-ft-F°): 0.67
Heat capacity asphalt (BTU/lb-F°): 0.23

**Asphalt Mix**

Number of temperatures: 5
Number of frequencies: 6

| Temperature °F | Mixture E* (psi) | | | | | |
|---|---|---|---|---|---|---|
| | 0.1 | 0.5 | 1 | 5 | 10 | 25 |
| **39.2** | 1289966 | 1465848 | 1691053 | 1944956 | 2086126 | 2290194 |
| **50** | 910305 | 1138609 | 1325340 | 1610934 | 1740211 | 1947905 |
| **77** | 289350 | 472997 | 575698 | 831260 | 958603 | 1151165 |
| **104** | 58837 | 114904 | 160528 | 304144 | 385075 | 523925 |
| **127.4** | 20870 | 55428 | 79864 | 166782 | 219385 | 304343 |

**Asphalt Binder**

Option: Superpave binder test data

| Temperature °F | Angular frequency = 10 rad/sec | |
|---|---|---|
| | G*, psi | Delta (°) |
| **114.8** | 42069 | 75 |
| **125.6** | 17537 | 78 |
| **136.4** | 7754 | 81 |
| **147.2** | 3481 | 83 |
| **156.2** | 1646 | 86 |
| **167** | 815 | 87 |
| **177.8** | 425 | 88 |

**Layer 5 -- JPCP (existing)**

**General Properties**

| | |
|---|---|
| Material type: | JPCP (existing) |
| Layer thickness (in): | 10 |
| Unit weight (pcf): | 150 |
| Poisson's ratio: | 0.2 |

**Strength Properties**

| | |
|---|---|
| Elastic/resilient modulus (psi): | 35000 |

**Thermal Properties**

| | |
|---|---|
| Thermal conductivity (BTU/hr-ft-F°) : | 1.25 |
| Heat capacity (BTU/lb-F°): | 0.28 |

**Layer 6 -- A-2-7**

| | |
|---|---|
| Unbound Material: | A-2-7 |
| Thickness(in): | 12 |

**Strength Properties**

| | |
|---|---|
| Input Level: | Level 3 |
| Analysis Type: | ICM inputs (ICM Calculated Modulus) |
| Poisson's ratio: | 0.35 |
| Coefficient of lateral pressure,Ko: | 0.5 |
| Modulus (input) (psi): | 25000 |

**ICM Inputs**

Gradation and Plasticity Index

| | |
|---|---|
| Plasticity Index, PI: | 29 |
| Liquid Limit (LL) | 50 |
| Compacted Layer | No |
| Passing #200 sieve (%): | 27.4 |
| Passing #40 | 37.1 |
| Passing #4 sieve (%): | 55.4 |
| D10(mm) | 0.00112 |
| D20(mm) | 0.01255 |
| D30(mm) | 0.1349 |
| D60(mm) | 5.73 |
| D90(mm) | 26.71 |

| Sieve | Percent Passing |
|---|---|
| **0.001mm** | |
| **0.002mm** | |
| **0.020mm** | |
| **#200** | 27.4 |
| **#100** | |
| **#80** | 32 |
| **#60** | |
| **#50** | |
| **#40** | 37.1 |
| **#30** | |
| **#20** | |
| **#16** | |
| **#10** | 47.6 |
| **#8** | |
| **#4** | 55.4 |
| **3/8"** | 72.4 |
| **1/2"** | 78.1 |
| **3/4"** | 85.3 |
| **1"** | 89.1 |
| **1 1/2"** | 94.6 |
| **2"** | 97 |
| **2 1/2"** | |
| **3"** | |
| **3 1/2"** | 100 |
| **4"** | 100 |

Calculated/Derived Parameters

| | |
|---|---|
| Maximum dry unit weight (pcf): | 120.8 (derived) |
| Specific gravity of solids, Gs: | 2.70 (derived) |
| Saturated hydraulic conductivity (ft/hr): | 6.832e-006 (derived) |
| Optimum gravimetric water content (%): | 10.6 (derived) |
| Calculated degree of saturation (%): | 72.4 (calculated) |

Soil water characteristic curve parameters: Default values

| Parameters | Value |
|---|---|
| **a** | 100.49 |
| **b** | 0.73434 |
| **c** | 0.26805 |
| **Hr.** | 500 |

### Layer 7 -- A-2-7

Unbound Material: A-2-7
Thickness(in): Semi-infinite

**Strength Properties**

| | |
|---|---|
| Input Level: | Level 3 |
| Analysis Type: | ICM inputs (ICM Calculated Modulus) |
| Poisson's ratio: | 0.35 |
| Coefficient of lateral pressure,Ko: | 0.5 |
| Modulus (input) (psi): | 25000 |

**ICM Inputs**

Gradation and Plasticity Index

| | |
|---|---|
| Plasticity Index, PI: | 29 |
| Liquid Limit (LL) | 50 |
| Compacted Layer | No |
| Passing #200 sieve (%): | 27.4 |
| Passing #40 | 37.1 |
| Passing #4 sieve (%): | 55.4 |
| D10(mm) | 0.00112 |
| D20(mm) | 0.01255 |
| D30(mm) | 0.1349 |
| D60(mm) | 5.73 |
| D90(mm) | 26.71 |

| Sieve | Percent Passing |
|---|---|
| **0.001mm** | |
| **0.002mm** | |
| **0.020mm** | |
| **#200** | 27.4 |
| **#100** | |
| **#80** | 32 |
| **#60** | |
| **#50** | |
| **#40** | 37.1 |
| **#30** | |
| **#20** | |
| **#16** | |
| **#10** | 47.6 |
| **#8** | |
| **#4** | 55.4 |
| **3/8"** | 72.4 |
| **1/2"** | 78.1 |
| **3/4"** | 85.3 |
| **1"** | 89.1 |
| **1 1/2"** | 94.6 |
| **2"** | 97 |
| **2 1/2"** | |
| **3"** | |
| **3 1/2"** | 100 |
| **4"** | 100 |

Calculated/Derived Parameters

| | |
|---|---|
| Maximum dry unit weight (pcf): | 120.8 (derived) |
| Specific gravity of solids, Gs: | 2.70 (derived) |
| Saturated hydraulic conductivity (ft/hr): | 6.832e-006 (derived) |
| Optimum gravimetric water content (%): | 10.6 (derived) |
| Calculated degree of saturation (%): | 72.4 (calculated) |

Soil water characteristic curve parameters: Default values

| Parameters | Value |
|---|---|
| **a** | 100.49 |
| **b** | 0.73434 |
| **c** | 0.26805 |
| **Hr.** | 500 |